Electrochimica Acta 163 (2015) 260–270

Contents lists available at ScienceDirect

Electrochimica Acta

journal homepage: www.elsevier.com/locate/electacta

An Electrochemical Micro-System for Clozapine Antipsychotic Treatment Monitoring

Hadar Ben-Yoav [a,b,1,*], Sheryl E. Chocron [a,c], Thomas E. Winkler [a,c], Eunkyoung Kim [d], Deanna L. Kelly [e], Gregory F. Payne [c,d], Reza Ghodssi [a,b,c,**]

[a] MEMS Sensors and Actuators Laboratory (MSAL), University of Maryland, College Park, MD 20742, United States
[b] Department of Electrical and Computer Engineering, Institute for Systems Research, University of Maryland, College Park, MD 20742, United States
[c] Fischell Department of Bioengineering, University of Maryland, College Park, MD 20742, United States
[d] Institute for Bioscience and Biotechnology Research, University of Maryland, College Park, MD 20742, United States
[e] Maryland Psychiatric Research Center, University of Maryland School of Medicine, Baltimore, MD 21228, United States

ARTICLE INFO

Article history:
Received 5 December 2014
Received in revised form 11 February 2015
Accepted 13 February 2015
Available online 17 February 2015

Keywords:
Therapeutic drug monitoring (TDM)
Antipsychotic clozapine
Lab-on-a-chip
Schizophrenia
Redox cycling system

ABSTRACT

Clozapine is the most effective antipsychotic medication for schizophrenia, but it is underutilized because of the inability to effectively monitor its treatment efficacy and side effects. In this work, we demonstrate the first analytical micro-system for real-time monitoring of clozapine serum levels. An electrochemical lab-on-a-chip is developed and integrated with a catechol-chitosan redox cycling system. The microfabricated device incorporates 4 electrochemical reaction chambers with the capability of analyzing microliter-volume samples. Integration of the catechol-chitosan film amplifies the clozapine oxidative signal and improves the signal-to-noise ratio, which addresses sensitivity and selectivity challenges. Optimization of the redox cycling system fabrication parameters and analysis of various electrochemical techniques and data processing approaches is implemented to maximize clozapine detection performance. The device is tested with buffer samples containing clozapine and demonstrates a sensitivity of 54 $\mu C\,mL\,cm^{-2}\,\mu g^{-1}$ and a limit-of-detection of 0.8 $\mu g\,mL^{-1}$, a sensing performance similar to a counterpart macro-scale benchtop system. Importantly, the feasibility to differentiate between 0.33 $\mu g\,mL^{-1}$ and 3.27 $\mu g\,mL^{-1}$ clozapine concentrations in human serum without any preceding dilution or filtering procedures is demonstrated, a significant step towards utilizing point-of-care testing micro-systems for schizophrenia treatment management. With these micro-systems, we envision more effective and safe treatment that will enable fewer visits to the clinicians, decrease costs and patient burden.

1. Introduction

Schizophrenia is one of the most challenging and complex neuropsychiatric disorders. It is a chronic illness that affects 1% of the worldwide population [1,2]. While a lifelong treatment with antipsychotics is recommended, approximately half of the schizophrenia population is not receiving appropriate care [3]. Clozapine (CLZ) is the most effective antipsychotic treatment for chronic and treatment refractory patients with schizophrenia [3–8]. It is one of the few antipsychotics whose efficacy has been predicted by blood measurement [9–14]. An optimal therapeutic range (0.350–1 $\mu g\,mL^{-1}$) has been identified for high efficacy and low toxicity [13]. Current pharmacologic guidelines recommended that CLZ blood levels be monitored for optimal therapeutic response [3]. In spite of its superior effectiveness and the recommended guidelines, CLZ is under-prescribed and underutilized in the United States [15–17]. In fact, CLZ is suggested to be the most under-used evidence-based treatment in psychiatry [18–21]. This underutilization is proposed to be related to the burden to the patients of repeated blood draws (weekly for the first six months) to monitor for agranulocytosis (severely lowered white blood cell count), a rare but dangerous side effect [22–24]. Furthermore, nonadherence to medications is a widespread problem, and is one of the more frequent reasons for relapse, re-hospitalization and

* Corresponding author at: Institute for Systems Research, Department of Electrical and Computer Engineering, University of Maryland, College Park, MD 20742, United States. Tel.: +1 301 405-2168; fax: +1 301 314 9920.
** Corresponding author at: Institute for Systems Research, Department of Electrical and Computer Engineering, University of Maryland, College Park, MD 20742, United States. Tel.: +1 301 405-8158; fax: +1 301 314 9920.
E-mail addresses: benyoav@umd.edu (H. Ben-Yoav), ghodssi@umd.edu (R. Ghodssi).
[1] ISE member.

http://dx.doi.org/10.1016/j.electacta.2015.02.112
0013-4686/

higher treatment costs in people with schizophrenia [25]. However, real-time monitoring of CLZ blood levels can be used to optimize treatment efficacy, reduce the risk of toxicity, and allow physicians to know if patients are adherent to their treatment or need interventions to support adherence.

Electrochemical lab-on-a-chip (LOC) sensing micro-systems provide numerous advantages in clinical diagnostics, environmental monitoring, and biomedical research fields [26–30]. These micro-systems have been rapidly adopted by a number of clinical diagnostics applications bringing benchtop methods to the point-of-care (POC) [31]. LOC devices have rarely been utilized in mental health applications [32–39]. The few electrochemical-based examples including neurotransmitter measurement [40,41], stress analysis [42], oxidative stress assessment [43], and antipsychotic drug monitoring [44]. In recent years, the electrochemical activity of CLZ [45,46] and its detection [47–53] have been investigated with macro-scale benchtop systems, a minority of which have analyzed CLZ in blood samples [45,53–57]. When translating analytical macro-scale technology into the micro-scale regime, a number of challenges arise. Sample preparation and mixing with other fluids, physical and chemical effects (e.g., capillary forces, surface roughness, chemical interactions of construction materials on reaction processes), and low signal-to-noise ratio are among the most important problems to overcome in analytical micro-systems [58]. Furthermore, the sensitivity and the specificity of these micro-systems when testing complex biological fluids (e.g., cerebrospinal fluid, serum, saliva, and urine) are deteriorated due to interference of other electro-active analytes and non-specific adsorption to the surface of the electrode [59]. These challenges may affect the performance of the device and limit its ability to sense low drug concentrations in biological fluids. Utilizing LOC technology for therapeutic drug monitoring (TDM) of CLZ in schizophrenia will provide frequent, real-time blood levels to maximize efficacy and minimize toxicity [22]. Such information will enable clinicians to manage CLZ treatment and to close the healthcare loop between clinicians and patients. No studies to date have developed miniaturized micro-systems designed for TDM of CLZ at the POC.

In this work, an electrochemical LOC for real-time monitoring of CLZ blood levels is presented. The device is designed for minimal preparation steps and utilizes a redox cycling system for CLZ signal amplification (Scheme 1). Lithography and thin film metal deposition technology is used to fabricate the device. The fabricated device is modified with a thin film consisting of the redox cycling system. This modification is based on a 2-step biofabrication process that entirely relies on electrical signals (i.e., chitosan electrodeposition and catechol electro-modification) (Scheme 1A). In these processes, phenolic molecules (e.g., catechol [60], melanin [61], and lignin derivatives [62]) are being used as the electronic materials for bio-electronic devices. Specifically, the catechol-chitosan redox cycling system has been demonstrated to detect CLZ [53,63–66] with capabilities for miniaturization and system integration [38,67–69]. It has also shown to be a stable film with a small signal loss due to slow overall biomaterial degradation [70]. With the catechol-chitosan redox cycling system, CLZ is oxidized on the surface of the electrode and continuously regenerated back to its reductive state (Scheme 1B; top left figure). This redox cycling mechanism significantly increases the generated CLZ oxidative current, amplifying CLZ electrochemical signal. Recharging of the redox cycling system is accomplished by the introduction of a ruthenium compound, which intermittently reduces the catechol into its original state (Scheme 1B; top right figure).

Here, we present the electrochemical validation and film optimization of the device, as well as the functionality and the limit of detection (LOD) of CLZ sensing. Additionally, we demonstrate the feasibility of differentiating between 0.33 and 3.27 $\mu g\,mL^{-1}$ CLZ concentrations in undiluted and unfiltered human serum, a first step towards reducing the burden and allowing more frequent CLZ blood monitoring for the patient and clinicians.

2. Experimental

2.1. Test solutions and instrumentation

All chemicals were purchased from Sigma–Aldrich. Phosphate buffered saline (PBS; pH 7.4) was prepared by dissolving a concentrated tablet with deionized (DI) water resulting in a solution of 0.01 $mol\,dm^{-3}$ phosphate buffer, 0.0027 $mol\,dm^{-3}$ potassium chloride, and 0.137 $mol\,dm^{-3}$ sodium chloride. All electrochemical tests were performed with a CHI660D single channel potentiostat and an 8-channel multiplexer (CH

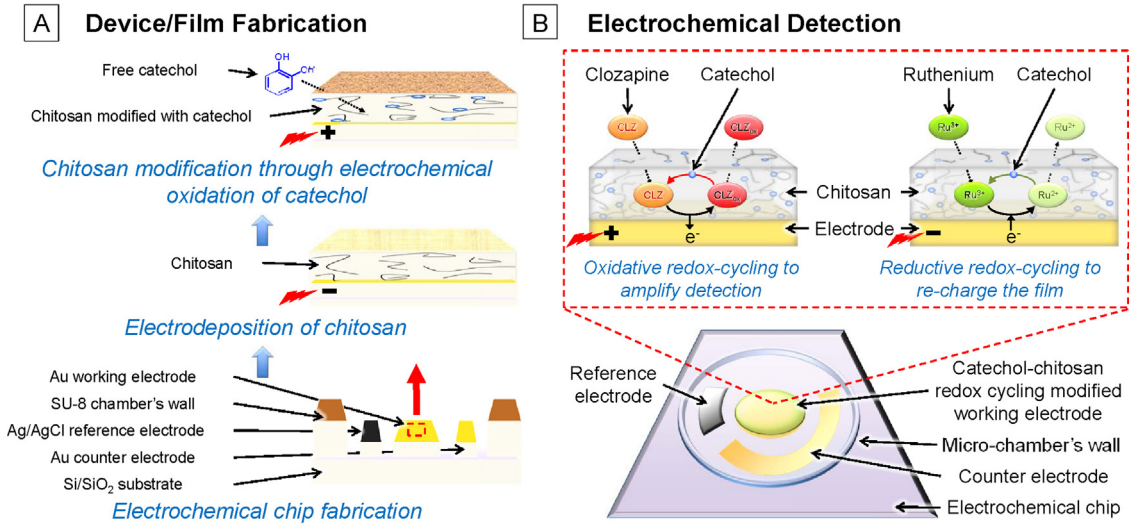

Scheme 1. Redox cycling system integrated in an LOC for CLZ detection. (A) Device/Film Fabrication. Catechol-chitosan redox cycling modified LOC fabrication methods (fabrication of the electrochemical chip, electrodeposition of chitosan on the working electrode, and modification of the chitosan film with catechol moieties). (B) Electrochemical Detection. 3-electrode electrochemical micro-chamber in the LOC modified with the catechol-chitosan redox cycling amplification film for CLZ sensing mechanism (top left) followed by recharging of the film with ruthenium (top right).

Instruments, Inc.). The potential values presented in this manuscript are all in reference to a Ag/AgCl half cell potential. Electrochemical validation of the device was performed by testing a mixture of 10 mmol dm^{-3} PBS with 100 mmol dm^{-3} sodium chloride along with 5 mmol dm^{-3} ferricyanide ($[Fe(CN)_6]^{3-}$) and 5 mmol dm^{-3} ferrocyanide ($[Fe(CN)_6]^{4-}$) yielding a solution with the reversible redox couple ions. A 28 μL volume was used with all solutions for testing with the device. The chitosan electrodeposition solution contained 1% dissolved chitosan in diluted HCl at pH 5–6. The catechol modification solution contained 5 mM of pyrocatechol dissolved in PBS solution. Additionally, 25 μmol dm^{-3} of hexaammineruthenium(III) chloride (Ru^{3+}; Ru) was dissolved in all tested solutions that indicate Ru. A film initialization step was carried out to fully reduce the chitosan-bound catechol residues and to consume all unbound catechol with a mixture of Ru and 25 μmol dm^{-3} of 1,1'-ferrocenedimethanol (Fc) dissolved in PBS. Commercial human serum (from human male AB plasma, USA origin, sterile-filtered) was divided into 1 mL aliquots and stored in −20 °C conditions. Prior to the experiment, the serum was thawed by horizontally lying down the tube on an ice bucket at room temperature.

2.2. Lab-on-a-chip design and fabrication

The design of the electrochemical LOC used in this work comprises four independent reaction chambers each containing an electrochemical cell. These cells are based on 3 individually addressed on-chip electrodes: working (WE; disk-shaped, 3 mm diameter) and counter (CE) gold electrodes, and a reference silver/silver chloride electrode (RE). The reaction chambers are defined in photoresist, resulting in round-shaped 9 mm diameter chambers with a sidewall height of 22 μm. The photoresist also passivates connecting wires on the chip from the tested solution.

The device is microfabricated on a silicon wafer (single-side polished prime grade quality, Ultrasil) modified with 1 μm of SiO_2 passivation layer, grown with a plasma-enhanced chemical vapor deposition (PECVD, Oxford Instruments) tool. A 20 nm thick Cr layer followed by a 200 nm thick Au layer are deposited (DC sputtering, AJA International, Inc.) on the wafer. The configuration of the WE, CE, and RE is patterned in Au using photolithography and thin film deposition technology, followed by subsequent patterning of the reaction chambers in SU-8 2015 photoresist (Microchem). Prior to the fabrication of the Ag/AgCl RE, an O_2 plasma step (IPC 4000, Branson) is applied to clean the surface of the electrodes from unwanted organic residues. The on-chip open Ag/AgCl RE is fabricated by a 2-step electrodeposition method: 1) Ag electroplating on the patterned Au electrode, 2) AgCl generation on the Ag electrode surface [71].

2.3. Lab-on-a-chip electrochemical validation

The unmodified LOC was evaluated by testing its electrochemical performance for the analysis of a known redox reaction. The ferrocyanide/ferricyanide reversible redox couple was used as a model system to characterize the Nernstian electrochemical response of the device. This was assayed by a conventional cyclic voltammetry (CV) technique using 0.02, 0.05, 0.08, 0.1, and 0.15 V s^{-1} scan rates (potential range between 0.4 V and −0.1 V; 2 cycles).

2.4. Catechol-chitosan redox cycling system fabrication, optimization, and characterization

The catechol-chitosan redox cycling film fabrication was modified from a recently published protocol [53]. Prior to the catechol-chitosan fabrication steps, the electrochemical activity of the device was verified with a ferrocyanide/ferricyanide solution. The open circuit potential (OCP) and the cyclic voltammogram response for each reaction chamber were recorded and compared to the expected standard reduction potential and reversible Nernstian behavior [72]. The Au WEs from all 4 reaction chambers (Fig. 1A) were simultaneously coated with chitosan by shorting of their contact pads and immersing the chip in chitosan solution while applying 6 A m^{-2} cathodic current. Platinum foil was used as both the counter and the pseudo-reference electrodes. The electrodeposition current was tested for an applied time of 15, 45, 60, and 90 seconds. This step resulted in a selective coating of chitosan on the WE regions of the chip (Fig. 1B and 1C). Despite of further rinsing step with PBS, some regions of the device other than the WE (e.g., the CE) were left with residues of chitosan (Fig. S1. CE's averaged roughness increased from 3.7 to 15.5 nm following the chitosan electrodeposition step). These residues can contribute to additional variability in the electrochemical measurement across chambers. The device was mounted onto an

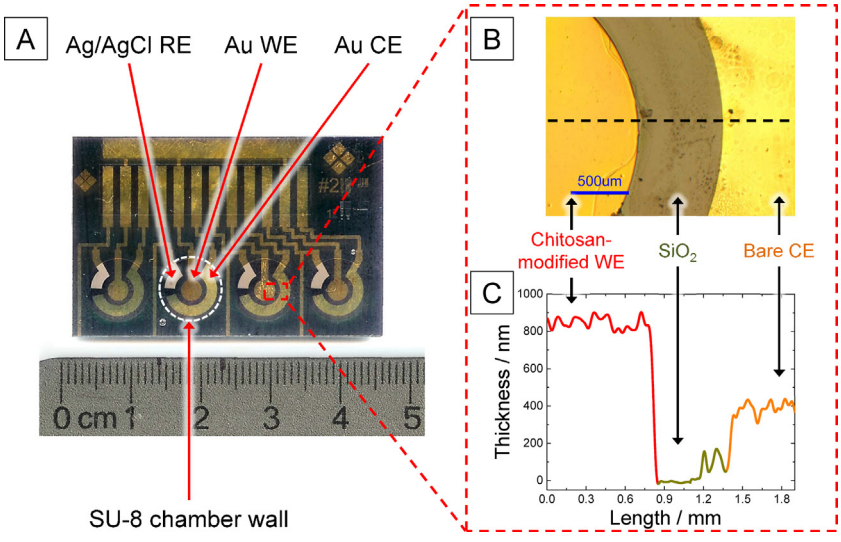

Fig. 1. (A) Image of the fabricated multi-chamber redox cycling integrated LOC (3 cm × 4.5 cm). (B) Microscope image and (C) cross-section thickness profile of a chitosan-modified WE and the CE (black dashed line indicates the location of the scanned profile).

electronic interface platform and connected to a multiplexer and a potentiostat. The chitosan films were further modified by placing a 5 mmol dm^{-3} catechol solution in each chamber and applying 0.6 V anodic potential to electrochemically oxidize the catechol. Catechol oxidation was applied for a duration of 30, 60, 120, 180, 210, 240, and 300 seconds. To clean the chip from unbound catechol, the chip was left in DI water for 5 minutes. The thickness of the chitosan-only and catechol-chitosan films was characterized using a surface profilometer (Dektak 6M, Veeco) followed by drying of the film with a N_2 gun.

2.5. Clozapine electrochemical detection assays

The multi-chamber device with unmodified WEs was used to characterize the influence of Ru on the CLZ measurement. PBS solutions with and without Ru were spiked with 0.5 (0.16), 1 (0.33), 5 (1.63), 10 (3.27), and 25 (8.17) μmol dm^{-3} (μg mL^{-1}) CLZ concentrations, and tested using a CV technique (potential range between −0.4 V and 0.7 V; a scan rate of 0.02 V s^{-1}; 2 cycles). Devices modified with different chitosan thicknesses and oxidized catechol densities were tested to optimize the fabrication steps of the catechol-chitosan film. Prior to each experiment, an initialization step was performed to reduce most of the catechol embedded on the chitosan film, charging the redox cycling system. Specifically, a CV technique (potential range between −0.4 V and 0.6 V; a scan rate of 0.02 V s^{-1}; 2 cycles) was used to cycle redox reactions with the initialization solution containing Ru as the catechol-reducing mediator and Fc as the catechol-oxidizing mediator. The sensing performance of CLZ was evaluated by testing a PBS solution containing Ru and CLZ with a CV technique (potential range between −0.4 V and 0.6 V; a scan rate of 0.02 V s^{-1}; 1 cycle).

The sensing performance of the device was compared between the bare and chitosan-modified Au WEs. Two chambers were modified with catechol-chitosan films and two chambers were modified with chitosan only. PBS solutions containing Ru and 0.16, 0.33, 1.63, 3.27, and 8.17 μg mL^{-1} CLZ concentrations were tested using CV technique (potential range between −0.4 V and 0.7 V; a scan rate of 0.02 V s^{-1}; 2 cycles) or differential pulse voltammetry (DPV) technique (potential sweep between 0 V and 0.7 V; potential increment of 0.001 V; amplitude of 0.05 V; pulse width of 0.2 s; sample width of 0.0167 seconds; pulse period of 0.5 s). Prior to each DPV test, the catechol-chitosan film was charged in the presence of Ru by applying a constant potential of −0.4 V for 120 s. Another set of partially modified devices (i.e., 2 chambers were modified with catechol-chitosan film and 2 chambers were modified with chitosan only) were used to test CLZ sensing in human serum. Commercial undiluted human serum was spiked with Ru and 0.33, 1.63, and 3.27 μg mL^{-1} CLZ concentrations right before testing. The CLZ-spiked serum samples were tested using a CV technique (potential range between −0.4 V and 0.6 V; a scan rate of 0.02 V s^{-1}; 1 cycle). All electrochemical tests were done in duplicates. Limit of Detection (LOD) values were determined as three standard deviation units above the calculated Y-intercept from a linear regression line [73].

3. Results and Discussion

3.1. Electrochemical characterization of the lab-on-a-chip with unmodified working electrodes

3.1.1. Electrochemical performance validation

The electrochemical performance of the LOC was validated with the commonly used redox couple ferrocyanide/ferricyanide. The resulting cyclic voltammograms represented reversible Nernstian characteristics for all the chambers in the device (Fig. 2A). Repeatable testing showed a steady open circuit potential (OCP) of 0.16600 ± 0.00035 V, representing a stable on-chip open reference electrode. Fig. 2B demonstrates a linear relationship between the current peaks and the square root of the scan rate, with slope values of $50 \times 10^{-5} \pm 4 \times 10^{-5}$ A $s^{1/2}$ $V^{-1/2}$ and $-49.0 \times 10^{-5} \pm 1.5 \times 10^{-5}$ A $s^{1/2}$ $V^{-1/2}$, intercept values of $16 \times 10^{-6} \pm 7 \times 10^{-6}$ A and $-20 \times 10^{-6} \pm 3 \times 10^{-6}$ A and R^2 values of 0.98 and 0.99, for the anodic and cathodic current peaks respectively.

As steady-state conditions cannot be expected during the electrochemical measurements in the LOC (steady state is true when $v << 8 \times 10^{-6}$ V s^{-1} [72]), currents that are resulted by linear

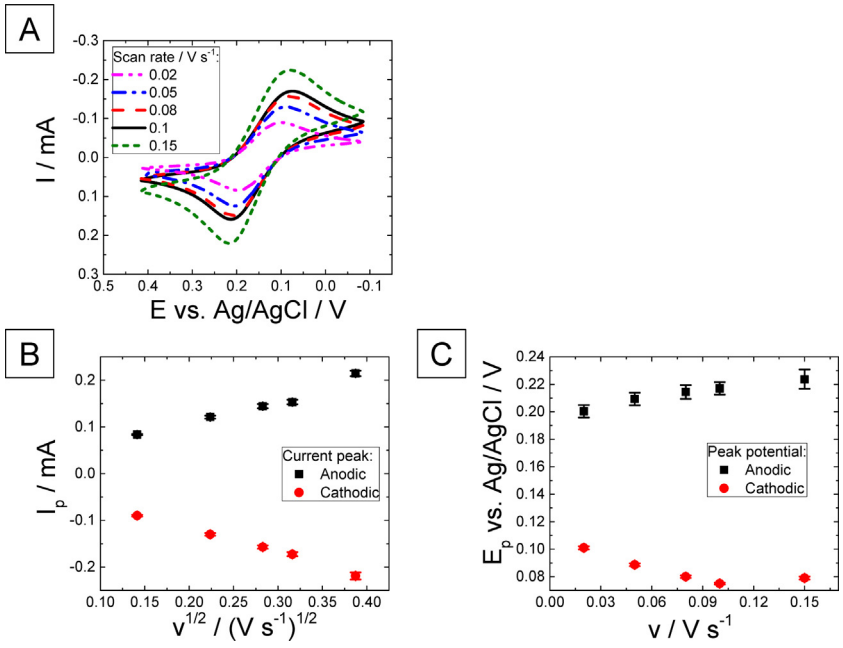

Fig. 2. Electrochemical validation of the unmodified LOC with a ferrocyanide/ferricyanide redox couple. (A) Representative cyclic voltammograms at scan rates of 0.02, 0.05, 0.08, 0.1, and 0.15 V s^{-1}. (B) The effect of the square root of the scan rate on the anodic and the cathodic peak currents. (C) The influence of the scan rate on the anodic and cathodic peak potentials.

diffusion will dominate those resulted by radial diffusion. Therefore it is valid to assume a theoretical relationship between the peak current and the scan rate described by the Randles-Sevcik equation [72] in order to calculate electrode active surface area values, as follows:

$$I_p = 0.4463\left(F^3/RT\right)^{1/2} n^{3/2} A D^{1/2} C^* \nu^{1/2} \quad (1)$$

Where I_p is the peak current [A], F [C mol^{-1}] is the Faraday constant, R [J mol^{-1} K^{-1}] is the universal gas constant, T [K] is the absolute temperature, n is the number of moles of electrons transferred in the cell reaction ($n = 1$ for a ferrocyanide/ferricyanide redox reaction), A is the active surface area of the electrode [cm^2], D [cm^2 s^{-1}] is the diffusion coefficient of the electro-active species (0.72×10^{-5} cm^2 s^{-1} for ferricyanide and 0.67×10^{-5} cm^2 s^{-1} for ferrocyanide [74]), C^* [mol cm^{-3}] is the bulk concentration of the electro-active species, and ν [V s^{-1}] is the linear potential scan rate. The averaged value of the active surface area of the electrode calculated from both the anodic and cathodic slopes was $A = 0.14 \pm 0.01$ cm^2. This value is approximately 2-fold bigger than the calculated area of the disk electrode. This variation can be mainly attributed to the additional active surface area of the electrode's wire connector that is not covered by the SU-8 passivation layer.

Fig. 2C shows a positive relationship between the scan rate and the anodic and the cathodic peak potentials, demonstrating increasing peak separation for larger scan rates. The trends for both reactions suggest that the sweep of the potential is not linear anymore due to an increased potential drop at the interface of the electrode. Such potential drop is resulted by uncompensated resistance and may be dominant at a microliter volume solution. Higher currents that are generated at faster scan rates increase this potential drop, causing the peak potential to be a function of the scan rate. As these limitations are common and can be compensated in micro-scale electrochemical devices, the electrochemical performance of the device was validated.

3.1.2. Clozapine electrochemical oxidation

The effect of Ru on the electrochemical oxidation of CLZ was tested with a bare gold WE in the LOC. Fig. 3 shows CVs of PBS solutions containing 0, 3.27, and 8.17 μg mL^{-1} CLZ, in the presence and absence of Ru. When Ru was absent, increasing concentration-dependent anodic ($E_p = 0.33$ V) and cathodic ($E_p = 0.27$ V) currents of CLZ were shown (Fig. 3A). When Ru was introduced to the sample, a sharp anodic peak became apparent at 0.43 V (Fig. 3B). This peak partially masked the CLZ anodic peak current. This anodic reaction was also present when no CLZ was added to the sample, suggesting that Ru may be involved in overlapping the electrochemical reaction of CLZ.

These results are significantly different from the previous study with buffered solution containing lower chloride ions concentrations [53], which did not show this peak in the presence of Ru, suggesting that chloride ions are also involved in the reaction. A possible explanation can be an electrochemical reaction between Ru and chloride ions. For example, solid ruthenium (reduced from ruthenium(II); $E^O = 0.23$ V) can be oxidized in the presence of chloride ions resulting in ruthenium trichloride at an $E^O = 0.46$ V. In the current LOC scheme, it is necessary to perform the test in the presence of chloride ions to maintain a stable half cell potential for the on-chip open Ag/AgCl reference electrode. Additionally, the presence of chloride ions better simulates the levels present in normal human serum, ranging between 100 to 110 mmol dm^{-3} of chloride ions [75,76]. Identifying the source of electrochemical reactions that occur at potentials adjacent to the CLZ standard reduction potential will help isolating the signal from CLZ oxidation.

3.2. Catechol-chitosan redox cycling system integration

3.2.1. Clozapine anodic current amplification

The ability of the catechol-chitosan modified LOC to amplify CLZ signal was studied. Fig. 3B (8.17 μg mL^{-1} CLZ concentration curve) and Fig. 4 show CVs of CLZ measured with bare electrodes

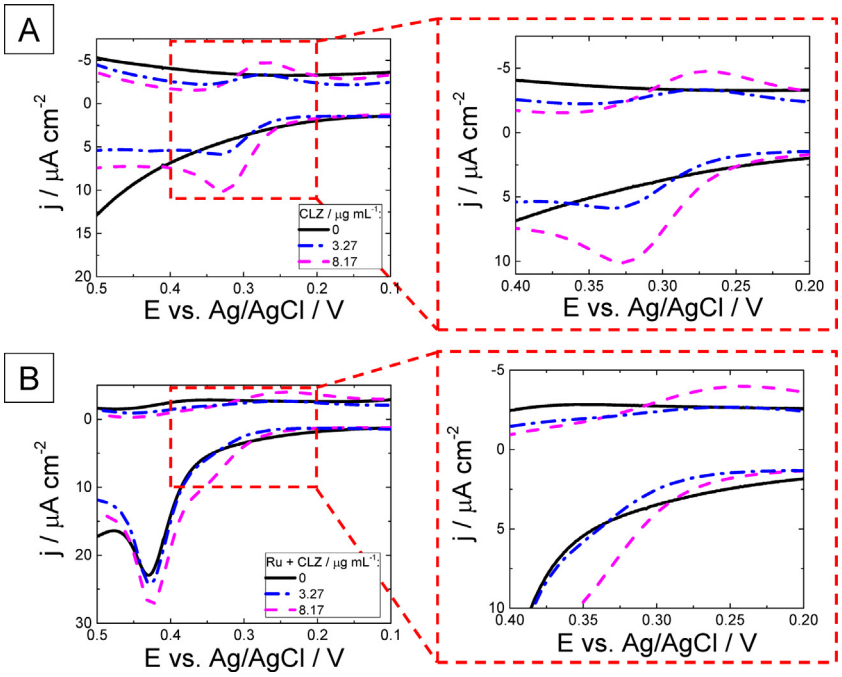

Fig. 3. CVs of 0 μg mL^{-1} (solid black), 3.26 μg mL^{-1} (dot-dashed blue), and 8.17 μg mL^{-1} (dashed magenta) CLZ concentrations in the absence (A) and the presence (B) of Ru in PBS solutions. Right-hand graphs present inside view of the CLZ anodic peak current density range. (For interpretation of the references to color in this figure legend, the reader is referred to the web version of this article.)

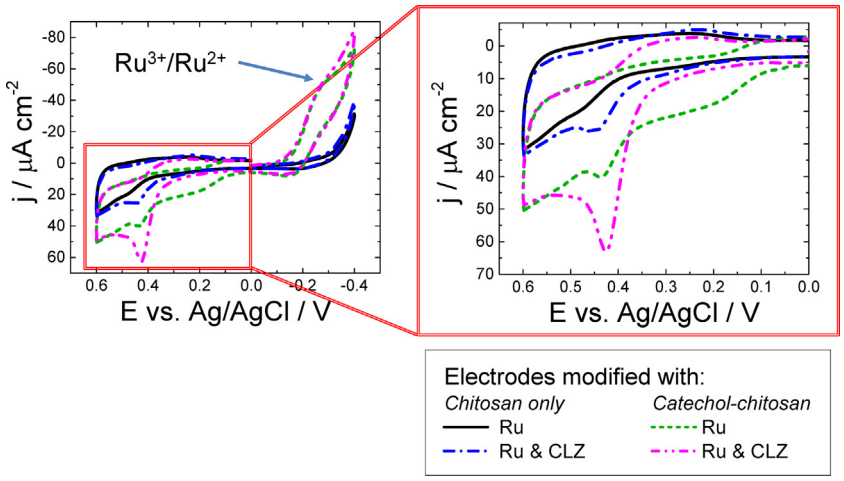

Fig. 4. Cyclic voltammograms of PBS solution with and without CLZ measured with electrodes modified with either catechol-chitosan (without CLZ – dashed green; with CLZ – dot-dot-dashed magenta) or chitosan only (without CLZ – solid black; with CLZ – dot-dashed blue). Magnified graph presents the oxidative region of the cyclic voltammogram. CLZ concentration was 8.17 µg mL^{-1}. (For interpretation of the references to color in this figure legend, the reader is referred to the web version of this article.)

and electrodes modified with catechol-chitosan and chitosan films, respectively. The overall anodic currents measured with catechol-chitosan modified electrodes were larger than their counterparts measured with either bare or chitosan-modified electrodes. These amplified currents are due to the redox cycling system, which continuously regenerates CLZ and other oxidized and reversible electro-active species in the sample. Despite the amplified current of CLZ, its anodic peak wasn't differentiable in the current setup from other anodic reactions in the system. Therefore, different data processing approaches were evaluated and assessed with respect to their effect on the sensing performance.

Evaluating the electrochemical current generated at the expected oxidation potential of CLZ provides a specific approach as opposed to calculating the total electrochemical charge for a range of potentials. On the other hand, the calculated charge essentially integrates a set of CLZ oxidative currents at different potentials, accumulates the whole CLZ oxidation capacity in the system, and eventually obtains higher signals. However, during this process, oxidation capacities of other electro-active species can be accumulated as well, which may contribute to higher background signals. Such background signals can be quantified and subtracted by the analysis of control samples (e.g., negative control without CLZ) and transducers (e.g., bare or chitosan-only modified sensor). The electrochemical charge was calculated for 4 different sections of the CV signal (Fig. 5) to evaluate which region better correlates to CLZ sensing: 1) Q_{r_red} for cathodic charge at $E < 0$ V, 2) Q_{r_ox} for anodic charge at $E < 0$ V, 3) Q_{o_ox} for anodic charge at $E > 0$ V, and 4) Q_{o_red} for cathodic charge at $E > 0$ V. Two different data subtraction methods were used to process the charge values (Eqs. (2) and (3)):

$$\text{“Sequential testing” approach: } Q_i^* = \left(Q_{i,with\,CLZ} - Q_{i,without\,CLZ}\right)_{electrode\,type} \quad (2)$$

$$\text{“Parallel testing” approach: } Q_i^* = \left(Q_{i,catechol-chitosan} - Q_{i,reference}\right)_{with\,CLZ} \quad (3)$$

where the annotation *i* is the relevant CV section (*r_red*; *r_ox*; *o_ox*; *o_red*), “electrode type” refers to bare, chitosan only and catechol-chitosan modified electrodes, and “reference” denotes the electrode used to measure the reference signal (either bare or chitosan only electrodes).

Table 1 compares the processed charge values for the two different data subtraction approaches. Results show higher charge magnitudes containing lower percentage errors with the “parallel testing” approach compared to “sequential testing” approach. Furthermore, Q_{r_red} and Q_{o_ox} yielded a higher magnitude of values than those processed using Q_{r_ox} and Q_{o_red} for both “parallel testing” and “sequential testing” approaches due to CLZ oxidation amplification and the related Ru reduction dominant in these sections. Within the “parallel testing” approach, using either the charge calculated from the bare or the chitosan-modified electrodes didn't have a significant effect on the values and errors calculated for $Q^*_{o\_ox}$ (50 µC and 10% vs. 45 µC and 13%). For $Q^*_{r\_red}$ values, the chitosan only electrode is suggested to be a better reference than the bare electrode by demonstrating higher anodic values and better percentage error (−90 µC and 17% vs. −60 µC and 27%). This analysis shows that “parallel testing” approach using $Q^*_{o\_ox}$ is better to identify CLZ detection.

Aside from analyzing data processing approaches, the methodological and design aspects of a POC testing device have to be taken into consideration. To provide accurate reference values for a “sequential testing” approach, two different solutions (i.e. a reference solution without CLZ followed by the sample with CLZ) will have to be introduced to the detection chamber and to be

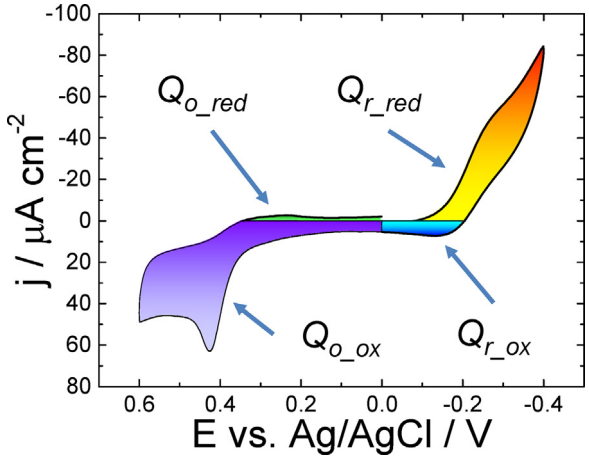

Fig. 5. Cyclic voltammogram charge sectioning diagram; Q_{r_red} (red-yellow) for cathodic charge at E < 0 V (Ru reduction), Q_{r_ox} (blue) for anodic charge at E < 0 V, Q_{o_ox} (purple) for anodic charge at E > 0 V (CLZ oxidation), and Q_{o_red} (green) for cathodic charge at E > 0 V. (For interpretation of the references to color in this figure legend, the reader is referred to the web version of this article.)

Table 1
Comparison of the different charge values between the 2 different data subtraction approaches.

Data subtraction approach	"Sequential testing"			"Parallel testing"	
Electrode type	bare	chitosan only	catechol-chitosan	Reference = bare	Reference = chitosan only
$Q^*_{r\_red}$/μC	−13.0 ± 1.3	−4.0 ± 2.6	−3 ± 24	−60 ± 16	−90 ± 15
Percentage error/%	10	65	800	27	17
$Q^*_{r\_ox}$/μC	0.005 ± 0.020	0.06 ± 0.24	−0.9 ± 2.0	6.0 ± 1.5	4.0 ± 1.5
Percentage error/%	400	400	222	25	37.5
$Q^*_{o\_ox}$/μC	−5.0 ± 1.0	9 ± 5	9 ± 15	50 ± 5	45 ± 6
Percentage error/%	20	55	167	10	13
$Q^*_{o\_red}$/μC	0.003 ± 0.100	−1.4 ± 0.3	−2.0 ± 0.6	5.0 ± 0.3	3.6 ± 0.3
Percentage error/%	3,333	21	30	6	8

measured by the same electrode. For a "parallel testing" approach, only one solution (i.e. the tested sample with CLZ) will have to be introduced to the chamber while a differential test will be performed between the catechol-chitosan and chitosan only modified electrodes. Previous experience with the catechol-chitosan film showed that even though the system is highly repeatable in buffered solutions, introduction of human serum samples in consecutive tests resulted in fouling of the sensor with approximately 10% decrease of the signal [53]. From the results in Table 1 and the methodological and design considerations, the "parallel testing" approach would provide a sensitive LOC with minimal pretreatment steps. As both bare and chitosan only modified electrodes showed similar detection factor values, chitosan was chosen to be the reference signal. Utilizing electrodes coated with chitosan film provides possible future chemical modifications (e.g. moieties that are negatively charged to repulse CLZ or that can adsorb CLZ decreasing its diffusion coefficient). These modifications will interact with CLZ, selectively decreasing the reference electro-active charge generated by CLZ.

A comparison of the calculated "parallel testing" approach value for $Q^*_{o\_ox}$ (defined as CLZ detection factor) between macro-scale electrodes [53] and the LOC presented here showed higher values for the former (263 μC vs. 45 μC, respectively). However, when taking the surface area of the electrode into account, the charge density values were similar (468 $\mu C\,cm^{-2}$ vs. 450 $\mu C\,cm^{-2}$). Therefore, in spite of the macro-scale setup having electrodes that have approximately 5 times higher surface area and milliliter-sized solution volumes, the LOC device achieved the same CLZ detection factor with microliter-sized volume samples and in the presence of chloride ions.

3.2.2. Catechol-chitosan film optimization

The chitosan electrodeposition and catechol modification steps were optimized to maximize the ability of the LOC to detect CLZ. First, the influence of the electrodeposition duration on the resulting chitosan thickness was characterized (Fig. 6A). Results showed a positive linear relationship with a slope value of 14.00 ± 0.25 $nm\,s^{-1}$, an intercept value of 180 ± 15 nm and R^2 value of 0.99. Because the thickness values include the dried chitosan layer as well as the underlying Cr/Au electrode layers, the intercept value indicates the thickness of a bare electrode. The intercept value was smaller than expected (220 nm). This variation may be due remaining chitosan residues on the SiO_2 surface adjacent to the electrode. The linear relationship between chitosan thickness and electrodeposition step duration suggested good process control in the micro-chip level with expected deposition mechanism [77].

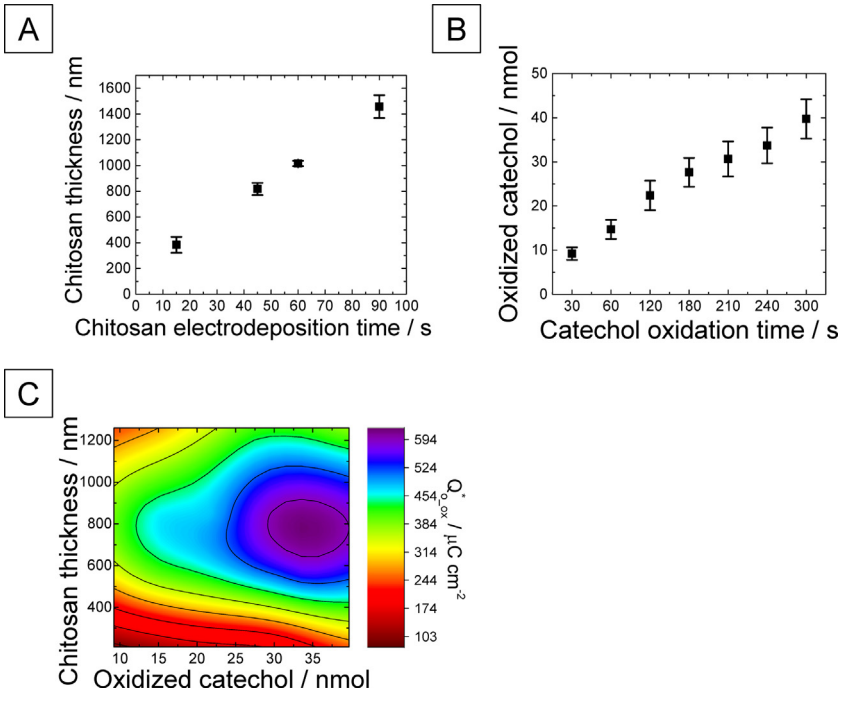

Fig. 6. Optimization of redox cycling film preparation. (A) The influence of the chitosan electrodeposition time on the thickness of the electrodeposited chitosan layer. (B) Oxidized catechol amount for increasing oxidation step duration. (C) The effect of the chitosan electrodeposition and the catechol modification steps on the CLZ detection factor.

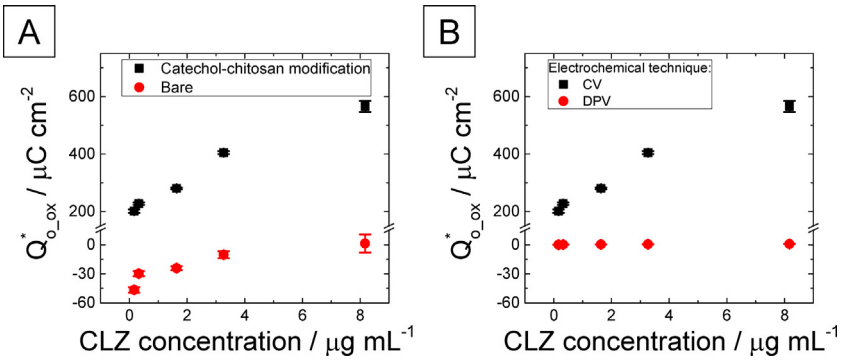

Fig. 7. CLZ dose response characteristics. (A) A comparison of the LOC integrated with the catechol-chitosan modification (black squares) and the bare gold electrode (red circles). (B) A comparison of electrochemical techniques measured with the LOC integrated with the catechol-chitosan modification: CV (black squares) and DPV (red circles). Negative values were observed for bare electrode due to higher chitosan reference charge values. (For interpretation of the references to color in this figure legend, the reader is referred to the web version of this article.)

CLZ detection was evaluated for various durations of chitosan electrodeposition (15, 45, 60, and 90 seconds) and catechol modification (30, 60, 120, 180, 210, 240, and 300 seconds). Fig. 6C shows a 2D contour representation of CLZ detection factor values tested with various chitosan thicknesses and oxidized catechol density (calculated from the generated charge during the catechol electrochemical oxidation step; Fig. 6B). An overall trend of increasing CLZ detection factor was demonstrated for increasing oxidized catechol densities. An optimized region was observed with a chitosan thickness of 800 nm and an oxidized catechol amount of 34 nmol (converted from the charge generated during the catechol oxidation step using Faraday's law), corresponding to a chitosan electrodeposition time of 60 seconds and a catechol modification time of 240 seconds, respectively.

3.3. Clozapine sensing performance with the catechol-chitosan redox cycling integrated lab-on-a-chip

The sensing performance of the LOC was characterized using different concentrations of CLZ (0.16, 0.33, 1.63, 3.27, and 8.17 μg mL^{-1}) in PBS solutions. Fig. 7A compares differently modified electrodes integrated in the LOC for the CLZ calibration curve obtained from CV results (Corresponding anodic current density peak values are presented in figure S2). Positive linear relationships were observed for the modified and the bare electrodes, with sensitivity values of 54 ± 7 μC mL cm^{-2} μg^{-1} and 7.0 ± 2.6 μC mL cm^{-2} μg^{-1}, and LOD values of 0.8 μg mL^{-1} and 2.1 μg mL^{-1}, respectively (Corresponding analysis of the anodic current density peak values of the modified electrode resulted in similar LOD values but inferior sensitivity; Fig. S3 and Table S1). The better sensitivity (8-fold higher) and better LOD (2-fold lower) measured with the catechol-chitosan modification compared to bare electrodes are related to the higher charge values achieved due to redox cycling. These higher charge values increase the signal-to-noise ratio and the selectivity of the sensor for CLZ.

DPV is an electrochemical technique that is commonly used in analytical applications due to decreased non-faradaic currents during measurements. Fig. 7B presents the effect of electrochemical techniques on the sensing performance of the LOC integrated with the catechol-chitosan film (Corresponding anodic current density peak values are presented in Fig. S2). A positive linear dose response for the DPV technique was obtained with sensitivity and LOD values of 0.100 ± 0.013 μC mL cm^{-2} μg^{-1} and 0.9 μg mL^{-1}, respectively. CV demonstrated better sensitivity (540-fold higher) than DPV even though higher non-faradaic currents were measured. As DPV is a preferred technique for electrochemical reaction analysis, CV will be a better choice for sensing purposes due to the higher accumulated charge. On the other hand, as Ru seems to interfere with CLZ detection, DPV was used here to test CLZ in the absence of Ru as opposed to CV. Negative control measurement showed a small anodic current peak at 0.34 V which may be due to Ru interference (Fig. S4). This suggests that Ru compounds may remain in the catechol-chitosan film due to the prior electrochemical charging step. Integration of methods to ensure that Ru does not remain in the film (e.g., soaking in DI for Ru diffusion out of the film) will decrease potential interference, reduce background signal, and improve the sensing performance.

3.4. Clozapine detection in human serum

The ability of the redox cycling integrated LOC to detect CLZ in human serum with no sample preparation steps (dilution, filtration, etc.) was tested. Different concentrations of CLZ (0.33, 1.63 and 3.27 μg mL^{-1}) spiked into undiluted serum were analyzed with the device. The intensity of electrochemical current generated from commercial serum varied by a magnitude of order between batches (data not shown) [78]. Therefore, an additional pair of catechol-chitosan and chitosan- modified electrodes were used as an on-chip reference measurement subtracting the blank signal from serum with no consecutive tests that may foul the sensor (Eq. (4)):

$$Q^*_{o_ox,\ serum\ with\ CLZ} - Q^*_{o_ox,\ serum\ only} \quad (4)$$

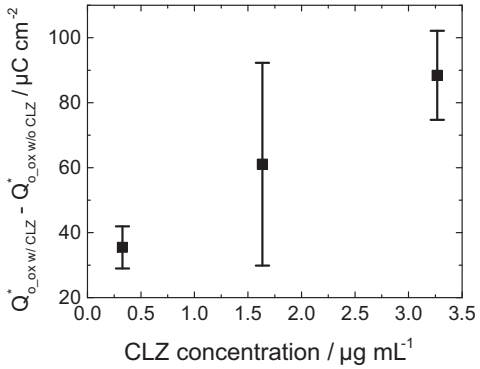

Fig. 8. Background subtracted detection factor values of human serum spiked with either 0.33, 1.63, or 3.27 μg mL^{-1} CLZ concentrations.

Fig. 8 shows the resulting subtracted values for different concentrations of CLZ-spiked serum. These results show increasing charge values with higher CLZ concentrations. A statistical analysis using an independent two-sample t-test demonstrated a significant difference between 0.33 and 3.27 $\mu g\,mL^{-1}$ CLZ concentrations with a p-value of 0.037 (significance level of 0.05). These results provided the feasibility of the device to differentiate between different concentrations of CLZ in untreated human serum samples. As these concentrations are close to the upper limit of the required clinical range for toxicity evaluation (i.e., 1 $\mu g\,mL^{-1}$), additional comprehensive characterization of the capability of the device to detect CLZ in serum will provide the required sensitivity and LOD values. For example, the variability of commercial serum samples will be addressed by acquiring samples directly from healthy subjects and characterizing the subject-to-subject electrochemical activity difference. Furthermore, the cross-reactivity of different electro-active species will be investigated to identify the major interferents.

4. Conclusions

In this work, we present a redox cycling integrated LOC for real time, electrochemical detection of CLZ. The microfabricated electrochemical device demonstrated highly repeatable and Nernstian behavior in multiple reaction chambers with microliter sample aliquots. Different electrochemical techniques, data processing approaches, and redox cycling film fabrication parameters were evaluated in order to optimize CLZ sensing and signal amplification. Studying the influence of the catechol-chitosan film fabrication process on physical and chemical reactions participating in the sensing mechanism will elucidate dominant phenomena that can be used to improve drug accessibility and limit ionic resistance in the system. The sensitivity and the LOD of the redox cycling integrated device were studied with buffered samples, providing crucial evidence of the sensor functionality. Finally, the feasibility of the device to differentiate between two concentrations of CLZ in human serum within the upper limit of the required clinical range was demonstrated.

These achieved characteristics demonstrate CLZ detection with a miniaturized redox cycling system for the first time. While macro-scale assays showed an 8-fold LOD improvement [53] and the recommended therapeutic CLZ blood levels are in the range of 0.35–1 $\mu g\,mL^{-1}$ [13], these accomplishments provide initial understanding of systems integration and dominant mechanisms in redox cycling integrated electrochemical micro-systems for analytical applications. Other redox cycling-integrated miniaturized detection assays demonstrated similar characteristics for other analytes [79–82]; for example, 10 $\mu mol\,dm^{-3}$ LOD of paracetamol was demonstrated by Goluch et al. [79]. Despite the better LOD and sensitivity of current commercial benchtop technologies for CLZ detection (e.g., liquid chromatography–tandem mass spectroscopy quantification method [83]), this miniaturized analytical device will allow treatment teams to perform analysis at the POC in a low cost, fast, and straightforward way aiming to guide CLZ dosages within the effective range, to decrease the patient's burden, and to personalize medical care.

This work is the first step in the device development and characterization towards portable micro-systems for rapid analysis of CLZ with minimal pretreatment steps. Aiming towards an assay with minimal pretreatment steps provides a simpler LOC paradigm that will achieve better overall systems integration capabilities. However, such a paradigm will suffer from limited sensitivity and LOD as sample pretreatment steps decrease the level of interference. A future study of CLZ detection in serum samples will provide additional information on the device performance with complex biological fluids. Such study will include possible variability and cross-reactivity parameters (e.g., electro-active species, patient-to-patient variability) interfering with the capability of the device to detect electrochemical signals generated by CLZ. Another direction will investigate other redox cycling schemes instead of the catechol-chitosan film, such as a 2-electrode configuration. As such a scheme will decrease the complexity of the fabricated device, other aspects will have to be taken into consideration during the design step (e.g., diffusion limitations due to the distance between electrodes, unstable half cell potential of the electrodes due to variations of the elector-active species concentrations). This novel application of portable analytical micro-systems for schizophrenia treatment monitoring will provide advantageous characteristics such as rapid, on-site, cost-effective, and straight-forward testing of the efficacy and the safety of the treatment at the POC (e.g., pharmacy, physician's office, clinic, hospital or at-home). With these devices the cost and burden of monitoring could be reduced, increasing the compliance of CLZ treatment among patients and prescribers and revolutionize the paradigm of how mental disorders are currently managed.

Acknowledgments

The authors would like to thank the Robert W. Deutsch Foundation, the Maryland Innovation Initiative (MII), and the NSF Grant No. DGE0750616 for financial support. The authors likewise appreciate the support of the Maryland NanoCenter and its FabLab. The authors wish to thank Professor Yosi Shacham-Diamand from Tel-Aviv University for providing experimental expertise in on-chip reference electrode fabrication. The authors wish to also thank the Bioengineering rotation students in MSAL: Bao-Ngoc Nguyen, Bharath Ramaswamy, Stephan Restaino, and Nicholas Woolsey and the undergraduate intern Gillian Costa for the useful discussions.

Appendix A. Supplementary data

Supplementary data associated with this article can be found, in the online version, at http://dx.doi.org/10.1016/j.electacta.2015.02.112.

References

[1] World Health Organization (WHO), http://www.who.int/mental_health/management/schizophrenia/en/.
[2] National Institute of Mental Health (NIMH), http://www.nimh.nih.gov/health/topics/schizophrenia/index.shtml.
[3] R.W. Buchanan, J. Kreyenbuhl, D.L. Kelly, J.M. Noel, D.L. Boggs, B.A. Fischer, S. Himelhoch, B. Fang, E. Peterson, P.R. Aquino, W. Keller, The 2009 Schizophrenia PORT psychopharmacological treatment recommendations and summary statements, Schizophrenia Bull. 36 (2010) 71.
[4] R.R. Conley, C.A. Tamminga, D.L. Kelly, C.M. Richardson, Treatment-resistant schizophrenic patients respond to clozapine after olanzapine non-response, Biol. Psychiat. 46 (1999) 73.
[5] J.M. Azorin, R. Spiegel, G. Remington, J.M. Vanelle, J.J. Pere, M. Giguere, I. Bourdeix, A double-blind comparative study of clozapine and risperidone in the management of severe chronic schizophrenia, Am. J. Psychiat. 158 (2001) 1305.
[6] R.W. Breier, B. Kirkpatrick, O.R. Davis, D. Irish, A. Summerfelt, W.T. Carpenter Jr., Effects of clozapine on positive and negative symptoms in outpatients with schizophrenia, Am. J. Psychiat. 151 (1994) 20.
[7] J. Kane, G. Honigfeld, J. Singer, H. Meltzer, Clozapine for the treatment-resistant schizophrenic. a double-blind comparison with chlorpromazine, Arch. Gen. Psychiat. 45 (1988) 789.
[8] J. Volavka, P. Czobor, B. Sheitman, J.P. Lindenmayer, L. Citrome, J.P. McEvoy, T.B. Cooper, M. Chakos, J.A. Lieberman, Clozapine, risperidone, and haloperidol in the treatment of patients with chronic schizophrenia and schizoaffective disorder, Am. J. Psychiat. 159 (2002) 255.
[9] D.J. Freeman, L.K. Oyewumi, Will routine therapeutic drug monitoring have a place in clozapine therapy? Clin. Pharmacokinet. 32 (1997) 93.
[10] C. Haring, U. Meise, C. Humpel, A. Saria, W.W. Fleischhacker, H. Hinterhuber, Dose-related plasma levels of clozapine: influence of smoking behaviour, sex and age, Psychopharmacology 99 (1989) S38.

[11] M. Hasegawa, R. Gutierrez-Esteinou, L. Way, H.Y. Meltzer, Relationship between clinical efficacy and clozapine concentrations in plasma in schizophrenia: effect of smoking, J. Clin. Psychopharm. 13 (1993) 383.
[12] P.J. Perry, K.A. Bever, S. Arndt, M.D. Combs, Relationship between patient variables and plasma clozapine concentrations: a dosing nomogram, Biol. Psychiat. 44 (1998) 733.
[13] A. Stark, J. Scott, A review of the use of clozapine levels to guide treatment and determine cause of death, Aust. NZ. J. Psychiat. 46 (2012) 816.
[14] B. Warner, L. Alphs, J. Schaedelin, T. Koestler, Clozapine and sudden death, Lancet 355 (2000) 842.
[15] R.R. Conley, D.L. Kelly, T.J. Lambert, R.C. Love, Comparison of clozapine use in maryland and in victoria, australia, Psychiat. Serv. 56 (2005) 320.
[16] H.Y. Meltzer, Clozapine: balancing safety with superior antipsychotic efficacy, Clin. Schizophr. Relat. Psychoses 6 (2012) 134.
[17] Y.-T. Xiang, C.-Y. Wang, T.-M. Si, E.H. Lee, Y.-L. He, G.S. Ungvari, H.F. Chiu, N. Shinfuku, S.-Y. Yang, M.-Y. Chong, Clozapine use in schizophrenia: findings of the research on asia psychotropic prescription (REAP) studies from 2001 to 2009, Aust. NZ. J. Psychiat. 45 (2011) 968.
[18] D.L. Kelly, J. Kreyenbuhl, R.W. Buchanan, A.K. Malhotra, Why not clozapine? Clin. Schizophr. Relat. Psychoses 1 (2007) 92.
[19] D.L. Kelly, H.J. Wehring, G. Vyas, Current status of clozapine in the United States, Shanghai Arch. Psychiatry 24 (2012) 110.
[20] J. Kane, Clozapine is under-utilized, Shanghai Arch. Psychiatry 24 (2012) 114.
[21] R. Joober, P. Boksa, Clozapine: a distinct, poorly understood and under-used molecule, J. Psychiatr. Neurosci. 35 (2010) 147.
[22] D.L. Kelly, H. Ben-Yoav, G.F. Payne, T.E. Winkler, S.E. Chocron, E. Kim V. Stock, G. Vyas, R.C. Love, H.J. Wehring, K.M. Sullivan, S. Feldman, F. Liu, R.P. McMahon, R. Ghodssi, The potential for applying technology to manage schizophrenia: point-of-care monitoring of clozapine, Submitted to Clin. Schizophr. Relat. Psychoses (2014).
[23] V.M. Stock, R.C. Love, H.J. Wehring, J. Kreyenbuhl, G. Vyas, C.M. Richardson, R. Ghodssi, H. Ben-Yoav, D.L. Kelly, Identifying barriers to the use of clozapine for schizophrenia, American Psychiatric Association Meeting, San Francisco, California, United States, 2013.
[24] D.L. Kelly, H. Ben-Yoav, V. Stock, T.E. Winkler, G.F. Payne, S.E. Chocron, E.G. Kim Vyas, R.C. Love, H.J. Wehring, K.M. Sullivan, S. Feldman, F. Liu, R.P. McMahon, R. Ghodssi, Development of a lab-on-a-chip biosensor for clozapine monitoring, 52nd Annual Meeting of the American College of Neuropsychopharmacology, Hollywood, Florida, United States, 2013.
[25] P. Thieda, S. Beard, A. Richter, J. Kane, An economic review of compliance with medication therapy in the treatment of schizophrenia, Psychiatr. Serv. 54 (2003) 508.
[26] C.D. Chin, V. Linder, S.K. Sia, Lab-on-a-chip devices for global health: past studies and future opportunities, Lab Chip 7 (2007) 41.
[27] H. Craighead, Future lab-on-a-chip technologies for interrogating individual molecules, Nature 442 (2006) 387.
[28] D. Figeys, D. Pinto, Lab-on-a-chip: a revolution in biological and medical sciences, Anal. Chem. 72 (2000) 330A.
[29] M.I. Mohammed, M.P.Y. Desmulliez, Lab-on-a-chip based immunosensor principles and technologies for the detection of cardiac biomarkers: a review, Lab Chip 11 (2011) 569.
[30] B.H. Weigl, R.L. Bardell, C.R. Cabrera, Lab-on-a-chip for drug development, Adv. Drug Deliver. Rev. 55 (2003) 349.
[31] V. Gubala, L.F. Harris, A.J. Ricco, M.X. Tan, D.E. Williams, Point of care diagnostics: status and future, Anal. Chem. 84 (2011) 487.
[32] M. Yamaguchi, T. Kanemori, M. Kanemaru, N. Takai, Y. Mizuno, H. Yoshida, Performance evaluation of salivary amylase activity monitor, Biosens. Bioelectron. 20 (2004) 491.
[33] V. Shetty, C. Zigler, T.F. Robles, D. Elashoff, M. Yamaguchi, Developmental validation of a point-of-care, salivary alfa-amylase biosensor, Psychoneuroendocrinology 36 (2011) 193.
[34] J. Nielsen, D. Thode, E. Stenager, K.Ø. Andersen, U. Sondrup, T.N. Hansen, A.M. Munk, S. Lykkegaard, A. Gosvig, I. Petrov, P. le Quach, Hematological clozapine monitoring with a point-of-care device: a randomized cross-over trial, Eur. Neuropsychopharm. 22 (2012) 401.
[35] J.H. Kim, D. Diamond, K.T. Lau, Optical device for non-invasive monitoring of lithium in bipolar disorder patients, in: Á. Jobbágy (Ed.), 5th European Conference of the International Federation for Medical and Biological Engineering, vol. 37, Springer, Berlin, Heidelberg, 2012, pp. 979.
[36] T.F. Robles, V. Shetty, C.M. Zigler, D.A. Glover, D. Elashoff, D. Murphy, M. Yamaguchi, The feasibility of ambulatory biosensor measurement of salivary alpha amylase: relationships with self-reported and naturalistic psychological stress, Biol. Psychol. 86 (2011) 50.
[37] V.K. Varadan, Nanotechnology based point-of-care diagnostics and therapeutics for neurological and cardiovascular disorders, in: 2010 IEEE Sensors (2010).
[38] P. Dykstra, J. Hao, S.T. Koev, G.F. Payne, L. Yu, R. Ghodssi, An optical MEMS sensor utilizing a chitosan film for catechol detection, Sensor. Actuat. B-Chem. 138 (2009) 64.
[39] J. Kirchheiner, L. Bertilsson, H. Bruus, A. Wolff, I. Roots, M. Bauer, Individualized medicine – implementation of pharmacogenetic diagnostics in antidepressant drug treatment of major depressive disorders, Pharmacopsychiatry 36 (2003) 235.
[40] A.A. Dawoud, T. Kawaguchi, Y. Markushin, M.D. Porter, R. Jankowiak, Separation of catecholamines and dopamine-derived dna adduct using a microfluidic device with electrochemical detection, Sensor. Actuat. B-Chem. 120 (2006) 42.
[41] M.J. Schöning, M. Jacobs, A. Muck, D.T. Knobbe, J. Wang, M. Chatrathi, S. Spillmann, Amperometric PDMS/glass capillary electrophoresis-based biosensor microchip for catechol and dopamine detection, Sensor. Actuat. B-Chem. 108 (2005) 688.
[42] M. Yamaguchi, M. Kanemaru, T. Kanemori, Y. Mizuno, Flow-injection-type biosensor system for salivary amylase activity, Biosens. Bioelectron. 18 (2003) 835.
[43] M.K. Hulvey, C.N. Frankenfeld, S.M. Lunte, Separation and detection of peroxynitrite using microchip electrophoresis with amperometric detection, Anal. Chem. 82 (2010) 1608.
[44] A. Floris, S. Staal, S. Lenk, E. Staijen, D. Kohlheyer, J. Eijkel, A. van den Berg, A prefilled, ready-to-use electrophoresis based lab-on-a-chip device for monitoring lithium in blood, Lab Chip 10 (2010) 1799.
[45] K. Farhadi, A. Karimpour, Electrochemical behavior and determination of clozapine on a glassy carbon electrode modified by electrochemical oxidation, Anal. Sci. 23 (2007) 479.
[46] J.M. Kauffmann, G.J. Patriarche, G.D. Christian, Electrochemical oxidation of derivatives of dibenzodiazepin. dibenzothiazepin and dibenzoxazepin, Anal. Lett. 12 (1979) 1217.
[47] T. Alizadeh, M. Akhoundian, A novel potentiometric sensor for promethazine based on a molecularly imprinted polymer (MIP): the role of MIP structure on the sensor performance, Electrochim. Acta 55 (2010) 3477.
[48] T. Alizadeh, M.R. Ganjali, M. Akhoundian, Synthesis and application of different nano-sized imprinted polymers for the preparation of promethazine membrane electrodes and comparison of their efficiencies, Int. J. Electrochem. Sci. 7 (2012) 7655.
[49] S.E. Haas, L. Brum, C. de Andrade, F.J. Azeredo, M. Pigatto, B.G. Silva Torres, S.S. Guterres, T.D. Costa, Highly sensitive LC-MS/MS method for the determination of clozapine in rat plasma: application to a preclinical pharmacokinetic study, J. Liq. Chromatogr. R. T. 35 (2012) 2873.
[50] M.H. Mashhadizadeh, E. Afshar, Electrochemical investigation of clozapine at TiO_2 nanoparticles modified carbon paste electrode and simultaneous adsorptive voltammetric determination of two antipsychotic drugs, Electrochim. Acta 87 (2013) 816.
[51] S.A. Mohajeri, G. Karimi, J. Aghamohammadian, M.R. Khansari, Clozapine recognition via molecularly imprinted polymers; bulk polymerization versus precipitation method, J. Appl. Polym. Sci. 121 (2011) 3590.
[52] R. Uřinovská, H. Brozmanová, P. Šištík, P. Šilhán, I. Kacířová, K. Lemr, M. Grundmann, Liquid chromatography–tandem mass spectrometry method for determination of five antidepressants and four atypical antipsychotics and their main metabolites in human serum, J. Chromatogr. B 907 (2012) 101.
[53] H. Ben-Yoav, T.E. Winkler, E. Kim, S.E. Chocron, D.L. Kelly, G.F. Payne, R. Ghodssi, Redox cycling-based amplifying electrochemical sensor for *in situ* clozapine antipsychotic treatment monitoring, Electrochim. Acta 130 (2014) 497.
[54] L. Hernandez, E. Gonzalez, P. Hernandez, Determination of clozapine by adsorptive anodic voltammetry using glassy carbon and modified carbon paste electrodes, Analyst 113 (1988) 1715.
[55] E. Hammam, A. Tawfik, M.M. Ghoneim, Adsorptive stripping voltammetric quantification of the antipsychotic drug clozapine in bulk form, pharmaceutical formulation and human serum at a mercury electrode, J. Pharmaceut. Biomed. 36 (2004) 149.
[56] T.B. Jarbawi, W.R. Heineman, Preconcentration of tranquilizers by adsorption/extraction at a wax-impregnated graphite electrode, Anal. Chim. Acta 186 (1986) 11.
[57] W. Jin, Q. Xu, W. Li, Determination of clozapine by capillary zone electrophoresis following end-column amperometric detection with simplified capillary/electrode alignment, Electrophoresis 21 (2000) 1415.
[58] A. Ríos, A. Escarpa, M.C. González, A.G. Crevillén, Challenges of analytical microsystems, TrAC-Trend. Anal. Chem. 25 (2006) 467.
[59] L.J. Kricka, Miniaturization of analytical systems, Clin. Chem. 44 (1998) 2008.
[60] E. Kim, Y. Xiong, Y. Cheng, H.-C. Wu, Y. Liu, B.H. Morrow, H. Ben-Yoav, R. Ghodssi, G.W. Rubloff, J. Shen, W.E. Bentley, X. Shi, G.F. Payne, Chitosan to connect biology to electronics: fabricating the bio-device interface and communicating across this interface, Polymers 7 (2015) 1.
[61] Y.J. Kim, W. Wu, S.E. Chun, J.F. Whitacre, C.J. Bettinger, Biologically derived melanin electrodes in aqueous sodium-ion energy storage devices, Proc. Natl. Acad. Sci. USA 110 (2013) 20912.
[62] G. Milczarek, O. Inganas, Renewable cathode materials from biopolymer/conjugated polymer interpenetrating networks, Science 335 (2012) 1468.
[63] H. Ben-Yoav, T.E. Winkler, S.E. Chocron, E. Kim, D.L. Kelly, G.F. Payne, R. Ghodssi, Micro-systems for point-of-care monitoring in mental health, Mid-Atlantic Micro/Nano Alliance Spring, Symposium, Baltimore, Maryland, United States, 2014, pp. 2014.
[64] H. Ben-Yoav, T.E. Winkler, S.E. Chocron, S.M. Restaino, G.R. Costa, E. Kim, D.L. Kelly, G.F. Payne, R. Ghodssi, 17th International Conference on Solid-State Sensors, Actuators and Microsystems (Transducers '13), Barcelona, Spain, 2013.
[65] H. Ben-Yoav, T.E. Winkler, E. Kim, D.L. Kelly, G.F. Payne, R. Ghodssi, in: 2013 MRS Spring Meeting (2013).
[66] H. Ben-Yoav, T.E. Winkler, S.E. Chocron, G.R. Costa, S.M. Restaino, N. Woolsey, E. Kim, D.L. Kelly, G.F. Payne, R. Ghodssi, 17th International Conference on Miniaturized Systems for Chemistry and Life Sciences (MicroTAS 2013), Freiburg, Germany, 2013.

[67] Y. Liu, X.W. Shi, E. Kim, L.M. Robinson, C.K. Nye, R. Ghodssi, G.W. Rubloff, W.E. Bentley, G.F. Payne, Chitosan to electroaddress biological components in lab-on-a-chip devices, Carbohyd. Polym. 84 (2011) 704.
[68] S.T. Koev, P.H. Dykstra, X. Luo, G.W. Rubloff, W.E. Bentley, G.F. Payne, R. Ghodssi, Chitosan: an integrative biomaterial for lab-on-a-chip devices, Lab Chip 10 (2010) 3026.
[69] E. Kim, Y. Liu, X.-W. Shi, X. Yang, W.E. Bentley, G.F. Payne, Biomimetic approach to confer redox activity to thin chitosan films, Adv. Funct. Mater. 20 (2010) 2683.
[70] T.E. Winkler, H. Ben-Yoav, S.E. Chocron, E. Kim, D.L. Kelly, G.F. Payne, R. Ghodssi, Electrochemical study of the catechol-modified chitosan system for clozapine treatment monitoring, Langmuir 30 (2014) 14686.
[71] H. Ben-Yoav, A. Biran, R. Pedahzur, S. Belkin, S. Buchinger, G. Reifferscheid, Y. Shacham-Diamand, A whole cell electrochemical biosensor for water genotoxicity bio-detection, Electrochim. Acta 54 (2009) 6113.
[72] A.J. Bard, L.R. Faulkner, Electrochemical Methods: Fundamentals and Applications, John Wiley & Sons Inc., New York, 2001.
[73] Analytical Methods Committee, Recommendations for the definition, estimation and use of the detection limit, Analyst 112 (1987) 199.
[74] S.J. Konopka, B. McDuffie, Diffusion coefficients of ferri- and ferrocyanide ions in aqueous media, Anal. Chem. 42 (1970) 1741.
[75] K. Arai, F. Kusu, N. Noguchi, K. Takamura, H. Osawa, Selective determination of chloride and bromide ions in serum by cyclic voltammetry, Anal. Biochem. 240 (1996) 109.
[76] O. Schales, S.S. Schales, A simple and accurate method for the determination of chloride in biological fluids, J. Biol. Chem. 140 (1941) 879.
[77] Y. Cheng, X. Luo, J. Betz, S. Buckhout-White, O. Bekdash, G.F. Payne, W.E. Bentley, G.W. Rubloff, In situ quantitative visualization and characterization of chitosan electrodeposition with paired sidewall electrodes, Soft Matter 6 (2010) 3177.
[78] European Collection of Cell Cultures (ECACC) and Sigma–Aldrich, Fundamental Techniques in Cell Culture Laboratory Handbook – 2nd Edition.
[79] E.D. Goluch, B. Wolfrum, P.S. Singh, M.A.G. Zevenbergen, S.G. Lemay, Redox cycling in nanofluidic channels using interdigitated electrodes, Anal. Bioanal. Chem. 394 (2009) 447.
[80] E. Kätelhön, B. Hofmann, S.G. Lemay, M.A.G. Zevenbergen, A. Offenhäusser, B. Wolfrum, Nanocavity redox cycling sensors for the detection of dopamine fluctuations in microfluidic gradients, Anal. Chem. 82 (2010) 8502.
[81] B. Wolfrum, M. Zevenbergen, S. Lemay, Nanofluidic redox cycling amplification for the selective detection of catechol, Anal. Chem. 80 (2008) 972.
[82] M.A.G. Zevenbergen, D. Krapf, M.R. Zuiddam, S.G. Lemay, Mesoscopic concentration fluctuations in a fluidic nanocavity detected by redox cycling, Nano Lett. 7 (2007) 384.
[83] R. Uřinovská, H. Brozmanová, P. Šištík, P. Šilhán, I. Kacířová, K. Lemr, M. Grundmann, Liquid chromatography-tandem mass spectrometry method for determination of five antidepressants and four atypical antipsychotics and their main metabolites in human serum, J. Chromatogr. B 907 (2012) 101.